Surge dynamics coupled to pore-pressure evolution in debris flows

S.B. Savage
Dept. of Civil Engineering & Applied Mechanics, McGill University, Montreal, Canada
R.M. Iverson
U.S. Geological Survey, Cascades Volcano Observatory, Vancouver, Washington

Keywords: debris flow, granular avalanche, slurry, pore pressure, consolidation, diffusion

ABSTRACT: Temporally and spatially varying pore-fluid pressures exert strong controls on debris-flow motion by mediating internal and basal friction at grain contacts. We analyze these effects by deriving a one-dimensional model of pore-pressure diffusion explicitly coupled to changes in debris-flow thickness. The new pore-pressure equation is combined with Iverson's (1997) extension of the depth-averaged Savage-Hutter (1989, 1991) granular avalanche equations to predict motion of unsteady debris-flow surges with evolving pore-pressure distributions. Computational results illustrate the profound effects of pore-pressure diffusivities on debris-flow surge depths and velocities.

1 INTRODUCTION

Debris flows are characterized by unsteady, surging motion of heterogeneous mixtures of solid and fluid constituents. Typically, the body of a debris-flow surge consists of a water-saturated, muddy, granular slurry liquefied by high pore-fluid pressure, whereas the snout of a debris-flow surge consists of unsaturated, coarse-grained, granular rubble that is pushed from behind by the liquefied slurry (Iverson 1997). Interaction of liquefied bodies with high-friction snouts gives debris-flow motion and deposition their key attributes. For example, lateral levees form where liquefied debris-flow bodies push aside the high-friction rubble that accumulates at debris-flow snouts (Fig. 1).

Coupling between mechanical processes at different scales generates the snout-and-body architecture that typifies debris flows. At small scales, debris agitation and grain interaction produce size segregation and selective transport of large clasts (Vallance & Savage 2000). These phenomena, together with selective retention of large clasts, lead to accumulations of coarse rubble at debris-flow snouts (Suwa 1988). The coarse rubble provides great frictional resistance because its high permeability facilitates ready drainage of pore fluid and dissipation of fluid pressure. In contrast, finer-grained slurries behind debris-flow snouts sustain high pore-fluid pressure owing to their low permeability and great compressibility, which produce low pore-pressure diffusivity.

In this paper we analyze how debris-flow motion and snout evolution are coupled to dif-

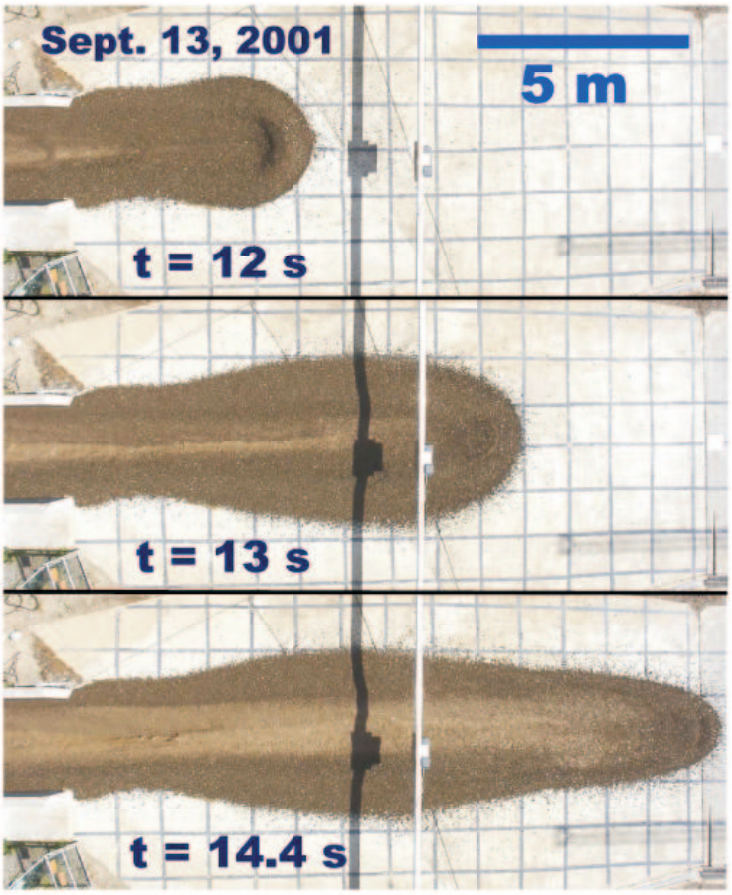

Figure 1: Aerial photographs of a debris-flow surge crossing the runout surface at the base of the U.S. Geological Survey debris-flow flume. The liquefied, fine-grained debris-flow body (light toned) interacts with the high-friction, coarse-grained snout (dark toned); "t" denotes elapsed time since the 9.4 m^3 debris flow was released as a homogenous mixture from the headgate 82.5m upslope. For more details see Iverson (2003).

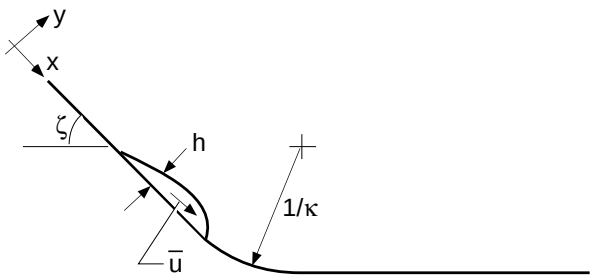

Figure 2: Definition sketch of coordinate system and geometry for flow of debris down a rough sloped surface.

fusion of pore-fluid pressure. Our analysis extends the approach of Iverson & Denlinger (2001), who assumed that pore-pressure evolution in debris flows obeys a homogeneous advective diffusion equation, unforced by changes in surge geometry. Here we incorporate forced pore-pressure diffusion by merging well-established theories for sediment consolidation and granular avalanche motion. The present analysis is based in part on the dry, cohesionless, granular avalanche theory of Savage & Hutter (1989, 1991) that was developed to predict the motion of a finite mass of granular material released from rest on slopes as shown in Figure 2. This theory assumes that the avalanche is long and thin such that depth-averaged equations of motion are sufficient to model the dynamics. A key assumption of this theory is that the ratio of shear to normal stress is almost constant over the depth of the granular flow (Savage & Sayed 1984, Savage & Hutter 1989). The shear stress at the bed τ is then obtained by multiplying the stress normal to the bed σ by a Coulomb bed friction coefficient; thus $\tau = \sigma \tan \delta$, where δ is the bed friction angle. The present analysis has a structure similar to this approach developed for dry materials. However, as in the debris-flow model of Iverson (1997) and Iverson & Denlinger (2001), we assume that Coulomb friction is mediated by pore-fluid pressure according to the Terzaghi effective-stress principle (Terzaghi 1963, Scott 1963). This formulation can be regarded as an extension of Hutchinson's (1986) one-dimensional, sliding-consolidation model for flow slides. His idea was that excess fluid pore pressures could be generated by the collapse of a metastable structure in loose, cohesionless materials. This high pore pressure can cause a temporary reduction of shear strength, thereby increasing the mobility of the debris. Because of the permeability of the solid matrix, consolidation occurs, and the excess pore pressures eventually decay with time. The resulting changes in the effective bed friction angle can significantly affect the dynamics of flow slides.

Our approach to analyzing debris-flow dynamics differs significantly from approaches that assume rheology determines flow resistance through a unique relation between stress and strain rate. In our formulation Coulomb friction implies no functional relationship between stress and strain rate. Instead, variable pore-fluid pressure mediates Coulomb friction and thereby determines flow resistance, which may vary with time and position. In this way, our model predicts the evolving character of flow resistance by using simple, well-established mechanical principles (momentum conservation, Coulomb friction, effective stress, and pore-pressure diffusion) rather than by assuming a debris-flow rheology.

2 ANALYSIS

As noted above, the present analysis is an extension of the depth-averaged Savage & Hutter (1989, 1991) dry granular flow model, Iverson's (1997) debris-flow model, and Hutchinson's (1986) sliding-consolidation model. The diffusion component of the analysis employs a simple, locally one-dimensional, integral method designed to determine basal pore pressure that can be incorporated into the Savage-Hutter depth-averaged granular flow model. The one-dimensional pore pressure diffusion model is a simple approach, but it is consistent with depth averaged granular flow model.

2.1 *Pore pressure diffusion model*

2.1.1 *Distributions of normal stress components over depth*

We first specify the various contributions to the normal stress over a liquid-solid layer of thickness h measured normal to the bed as shown in Figure 3. The coordinate y is measured

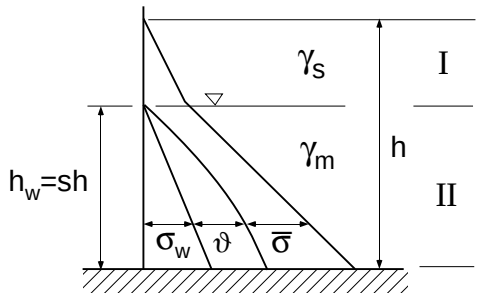

Figure 3: Normal stress contributions in solid-liquid mixture of total layer thickness h. The lower layer II of thickness $h_w = sh$ is fully saturated, whereas the upper layer I is dry.

perpendicular to the impermeable bed that is inclined at an angle ζ as shown in Figure 2. Consider the general case in which the total thickness h is divided into two layers (Fig. 3), a fully saturated lower region II of thickness $h_w = sh$ having a liquid-solid mixture specific gravity of γ_m, and a dry upper layer I of thickness $(1-s)h$ having a solids bulk specific gravity of γ_s. Thus, s is the fraction of the total layer thickness that is saturated.

We can express the component of the total normal stress σ that is perpendicular to the bed as the sum of the various components as follows

$$\sigma = \sigma_w + \vartheta + \overline{\sigma} \tag{1}$$

where σ_w is the hydrostatic water pressure, ϑ is the excess pore water pressure, and $\overline{\sigma}$ is the effective interparticle stress as shown in Figure 3.

Assuming that the bulk density of the solids ρ_s, the bulk density of the liquid-solid mixture ρ_m and the mass density of the water ρ_w are all constant, and defining g as the gravitational acceleration, we can determine that σ, the component of the normal stress perpendicular to the bed in the upper region I ($h_w \le y \le h$), is

$$\sigma = \rho_s \, g \, (h - y) \cos\zeta \, , \tag{2}$$

whereas, in the lower region II ($0 \le y \le h_w$) we find

$$\begin{aligned} \sigma - \sigma_w &= \left[\rho_s \, g \, (h - h_w) + (\rho_m - \rho_w) \, g \, (h_w - y)\right] \cos\zeta \\ &= \left[\frac{\rho_s}{\rho_m} \, (1-s) + \left(1 - \frac{\rho_w}{\rho_m}\right) \, s \, \left(1 - \frac{y}{h_w}\right)\right] \, \rho_m \, g \, h \, \cos\zeta \, . \end{aligned} \tag{3}$$

2.1.2 *Diffusion equation for excess pore pressure*

Let us start by considering a simplified example in which a layer of liquid-solid mixture has been sitting at rest on a horizontal bed for a considerable time such that any excess pore pressure has dissipated to zero and the total stress is due to the sum of the hydrostatic water pressure σ_w and the interparticle effective stress $\overline{\sigma}$. Both σ_w and $\overline{\sigma}$ vary linearly with depth when ρ_w, ρ_s and ρ_m are taken as constants. Now imagine that a collapse of the solid matrix or some other perturbation occurs so as to generate non-zero excess pore pressures as indicated by ϑ in Figure 3. It is of interest to describe how the excess pore pressure ϑ evolves or

diffuses with time. An appropriate excess pore pressure diffusion equation is required for this purpose. To derive this equation, we begin by assuming that both the interstitial fluid and solid particles are incompressible. The conservation of mass equation for the fluid (Gidaspow 1994) is then

$$\frac{\partial n}{\partial t} + \nabla \cdot (\mathbf{v}_f \, n) = 0 \,, \tag{4}$$

where n is the interstitial voids fraction, t is time and $\mathbf{v}_f$ is the velocity of the fluid. Similarly, the mass conservation equation for the solids component is

$$\frac{\partial \, (1-n)}{\partial t} + \nabla \cdot [\mathbf{v}_s \, (1-n)] = 0 \,, \tag{5}$$

where $\mathbf{v}_s$ is the velocity of the solids. Adding (4) and (5) yields

$$\nabla \cdot [n \, (\mathbf{v}_f - \mathbf{v}_s)] = -\nabla \cdot \mathbf{v}_s \,. \tag{6}$$

Using Darcy's Law (Bear 1979) we express $\mathbf{q}$, the specific discharge or superficial velocity of the pore fluid relative to the solids, as

$$\mathbf{q} = n \, (\mathbf{v}_f - \mathbf{v}_s) = -\frac{k}{\mu} \, \nabla \vartheta \,, \tag{7}$$

where k is the permeability, μ is the viscosity of the interstitial fluid and ϑ is the excess fluid pore pressure. Substituting (7) in (6), we obtain

$$\nabla \cdot \mathbf{v}_s = \nabla \cdot \left(\frac{k}{\mu} \, \nabla \vartheta \right) . \tag{8}$$

We can rewrite (5) as

$$\left[\frac{\partial n}{\partial t} + \mathbf{v}_s \cdot \nabla \, n \right] = \frac{dn}{dt} = (1-n) \nabla \cdot \mathbf{v}_s \,, \tag{9}$$

where dn/dt is the convective derivative of n. Combining (8) and (9) we obtain

$$\nabla \cdot \left(\frac{k}{\mu} \, \nabla \vartheta \right) = \frac{1}{(1-n)} \frac{dn}{dt} \,. \tag{10}$$

We now make the constitutive assumption that

$$\frac{1}{(1-n)} \frac{dn}{dt} = -\alpha \frac{d\overline{\sigma}}{dt} \,, \tag{11}$$

which implies the relation between effective stress $\overline{\sigma}$ and interstitial voids fraction n

$$\overline{\sigma} - \overline{\sigma}_o = \frac{1}{\alpha} \ln \left[\frac{1-n}{1-n_o} \right] , \tag{12}$$

where α is the mixture compressibility, and $\overline{\sigma}_o$ and n_o are reference values. Iverson (1997) has shown that this relation describes the volume change behavior of a variety of soils, slurries, and debris flows reasonably well. Combining (10), (11), and (1) yields

$$\frac{d\vartheta}{dt} = \frac{d}{dt}(\sigma - \sigma_w) + \frac{1}{\alpha} \nabla \cdot \left(\frac{k}{\mu} \, \nabla \vartheta \right) . \tag{13}$$

Let us write out the convective derivative

$$\frac{d}{dt} = \frac{\partial}{\partial t} + u_s \frac{\partial}{\partial x} + v_s \frac{\partial}{\partial y}\,, \tag{14}$$

where u_s and v_s are respectively x and y-components of the solids velocity. We now suppose that u_s, the x-component of the solids velocity, is nearly uniform over the depth and can be approximated by the depth-averaged streamwise velocity $\overline{u}\,(x,t)$. Using (14) we can write

$$\frac{d}{dt} \simeq \frac{\partial}{\partial t} + \overline{u}\frac{\partial}{\partial x} + v_s \frac{\partial}{\partial y} = \frac{\overline{\partial}}{\partial t} + v_s \frac{\partial}{\partial y}\,, \tag{15}$$

where

$$\frac{\overline{\partial}}{\partial t} = \frac{\partial}{\partial t} + \overline{u}\frac{\partial}{\partial x}\,, \tag{16}$$

is the time derivative in a system moving with the mean streamwise velocity in the x-direction. Consistent with the model of Savage & Hutter (1989, 1991), we take the surge to be long and thin such that the gradients in the y-direction perpendicular to the bed are much greater than those parallel to the bed along the x-direction; hence

$$\frac{1}{\alpha}\nabla \cdot \left(\frac{k}{\mu}\,\nabla\vartheta\right) \simeq D_v\,\frac{\partial^2\vartheta}{\partial\, y^2}\,, \tag{17}$$

where the pore pressure diffusivity $D_v = k/(\mu\alpha)$ is considered to have gradual variations in the streamwise direction. Making use of (15) and (17), and assuming that the vertical debris flow velocity $v \simeq v_s$, we can rewrite (13) as the forced excess pore pressure diffusion equation

$$\frac{\overline{\partial}\vartheta}{\partial t} + v\frac{\partial\vartheta}{\partial y} = \frac{\overline{\partial}}{\partial t}(\sigma - \sigma_w) + v\frac{\partial}{\partial y}(\sigma - \sigma_w) + D_v\,\frac{\partial^2\vartheta}{\partial\, y^2}\,. \tag{18}$$

Equation (18) has a locally one-dimensional form in a coordinate system moving with the local mean streaming velocity $\overline{u}$. The vertical debris flow velocity v that appears in (18) can be approximated in a coordinate system moving with the mean streaming velocity $\overline{u}$ (Savage & Hutter 1989, 1991) by

$$v \simeq \frac{y}{h}\frac{\overline{\partial}h}{\partial t}\,. \tag{19}$$

2.1.3 *Integral method for diffusion equation*

The basic idea of the present analysis is that we apply the one-dimensional diffusion equation (18) locally along the length of the surge. Equation (18) is a partial differential equation in time t and coordinate distance y referred to a Lagrangian system moving with the local mean streaming velocity $\overline{u}$. We now describe an integral method that is used to find solutions to (18). The y-dependence of (18) will be removed by integrating over the depth to produce an ordinary differential equation for the evolution of ϑ_b, the excess fluid pore pressure at the bed. This result will be used in conjunction with the momentum and continuity equations to describe the development of the debris flow surge that accounts for the effects of diffusion of the pore water pressure.

We introduce the dimensionless variables

$$\tilde{\vartheta} \;=\; \vartheta/\rho_m\, g\, H\, \cos\zeta, \quad (\tilde{\sigma} - \tilde{\sigma_w}) = (\sigma - \sigma_w)/\rho_m\, g\, H\, \cos\zeta\,,$$

$$\tilde{y} \;=\; y/H, \quad \tilde{h} = h/H, \quad \tilde{t} = t\sqrt{g/L}, \quad \text{and} \quad \tilde{D}_v = D_v\,\sqrt{(L/g)}/H^2\,, \tag{20}$$

where L and H are characteristic length scales in the x and y-directions respectively. Substituting (3), (19) and (20) in the diffusion equation (18), and dropping tildes yields the non-dimensional form of the forced excess pore pressure diffusion equation

$$\frac{\overline{\partial}\vartheta}{\partial t} + \frac{y}{h}\frac{\overline{\partial}h}{\partial t}\frac{\partial\vartheta}{\partial y} = A\,\frac{\overline{\partial}h}{\partial t} - \left[1 - \frac{\rho_w}{\rho_m}\right]\frac{y}{h}\frac{\overline{\partial}h}{\partial t} + D_v\,\frac{\partial^2\vartheta}{\partial\, y^2}\;, \tag{21}$$

where

$$A = \left[\frac{\rho_s}{\rho_m}\,(1-s) + \left(1 - \frac{\rho_w}{\rho_m}\right)\,s\right]\,.$$

Now we change variables from $(y,t) \rightarrow (\eta,t)$, where $\eta = y/s\,h$. Note that the derivatives, when transformed from the (y,t) to the (η,t) system, become

$$\frac{\partial}{\partial y} = \frac{\partial\eta}{\partial y}\frac{\partial}{\partial\eta} = \frac{1}{sh}\frac{\partial}{\partial\eta} \qquad \text{and} \qquad \frac{\overline{\partial}}{\partial t} = \frac{\overline{\partial}}{\partial t} - \frac{\eta}{h}\frac{\overline{\partial}h}{\partial t}\frac{\partial}{\partial\eta}\,, \tag{22}$$

Equation (21) then takes on the form

$$\frac{\overline{\partial}\vartheta}{\partial t} = \left[A\;-\left(1 - \frac{\rho_w}{\rho_m}\right)\,s\,\eta\right]\,\frac{\overline{\partial}h}{\partial t} + \frac{D_v}{s^2\,h^2}\,\frac{\partial^2\vartheta}{\partial\,\eta^2}\;, \tag{23}$$

which will be solved by a collocation or integral method of the kind sometimes used in boundary layer theory (Finlayson 1972). Note that (23) is a diffusion equation, but with a pore-pressure source term that depends on $\overline{\partial}h/\partial t$ and a time derivative that involves a convected coordinate. We proceed by assuming an excess pore pressure distribution for region II ($0 \le \eta \le 1$) of form

$$\vartheta(\eta,t) = \frac{6\,\vartheta_b(t)}{5}\,\left[(1-\eta) - \frac{1}{6}(1-\eta)^6\right]\;, \tag{24}$$

where ϑ_b is the excess pore pressure at the bed, $\eta = y/h_w$, and $h_w = h_w(t) = s\,h(t)$. This form for $\vartheta(\eta,t)$ satisfies the conditions at the lower and upper boundaries $\eta = 0, 1$

$$\vartheta(0,t) = \vartheta_b(t), \qquad \vartheta(1,t) = 0, \tag{25}$$

and the impermeable bed condition

$$v_f(0,t) = -\frac{k}{\mu}\,\frac{\partial\vartheta}{\partial\eta}\Big|_{\eta=0} = 0. \tag{26}$$

Equation (24) is a simple, one parameter representation of the excess pore pressure profile. One could assume a more complex profile, involving more parameters, in order to permit the profile shape to vary. However, numerical solutions of (23) for specified timewise variations of h indicated that the simple form given by (24) was adequate.

Substituting the profile (24) into the diffusion equation (23) and integrating over the depth for $0 \le \eta \le 1$, we obtain the equation for the evolution of excess pore pressure at the bed

$$\frac{\overline{\partial}\vartheta_b}{\partial t} = \frac{7}{4}\,\left[\left[A - \frac{s}{2}\left(1 - \frac{\rho_w}{\rho_m}\right)\right]\,\frac{\overline{\partial}h}{\partial t} - \frac{6\,D_v\,\vartheta_b}{5\,s^2\,h^2}\right]\;, \tag{27}$$

where again $\overline{\partial}/\partial t$ is the time derivative in a Lagrangian frame moving with the depth-averaged streamwise velocity $\overline{u}$.

2.2 *Depth-averaged momentum equation*

Because of lack of space, a detailed derivation for the depth-averaged streamwise momentum equation is not provided, but the final equation of motion is merely stated. We consider the simple case of flow over a plane bed having an inclination ζ, and debris that is fully saturated over the complete depth of material such that $s = 1$.

By following depth-averaging procedures similar to those used in Savage & Hutter (1989, 1991) and Iverson (1997) and using the excess pore pressure profile given by (24) we obtain the depth averaged streamwise momentum equation

$$\begin{aligned}\frac{\overline{\partial}\overline{u}}{\partial t} &= \frac{\partial \overline{u}}{\partial t} + \overline{u}\frac{\partial \overline{u}}{\partial x} = \sin\zeta - \tan\delta\ \mathrm{sgn}(\overline{u})\ \cos\zeta\ \left[1 - \frac{p_b}{h}\right] \\ &\quad -\epsilon\cos\zeta\ \left[k_{actpass}\frac{\partial h}{\partial x} + (1 - k_{actpass})\left(\frac{\rho_w}{\rho_m}\frac{\partial h}{\partial x} + \frac{4}{7h}\frac{\partial\,(h\,\vartheta_b)}{\partial x}\right)\right], \end{aligned} \tag{28}$$

where δ is the solids bed friction angle and the fluid shear stress at bed has been neglected, and the total bed pore pressure is defined as the sum of the excess pore pressure ϑ and the hydrostatic water pressure

$$p_b = \vartheta_b + \frac{\rho_w}{\rho_m}\, s\, h\,, \tag{29}$$

in which we take $s = 1$. Equations (28) and (29) have been expressed in terms of dimensionless variables defined by

$$(x, y, h) = (x^*/L,\ y^*/H,\ h^*/H)\,, \quad \epsilon = H/L,$$

$$(u, v, t) = \left(u^*/\sqrt{gL},\ v^*L/H\sqrt{gL},\ t^*\sqrt{g/L}\right) \qquad \vartheta_b = \frac{\vartheta_b^*}{\rho_m\, g\, H\ \cos\zeta}\,, \tag{30}$$

where the starred quantities represent physical variables. The coefficient $k_{actpass}$ that appears in (28) corresponds to an earth pressure coefficient discussed in Savage & Hutter (1989, 1991). It generates an active state of stress when the flow is diverging ($\partial\overline{u}/\partial x > 0$) and a passive state of stress when the flow is converging ($\partial\overline{u}/\partial x < 0$). Equation (28) is very similar to that derived by Iverson (1997) with the exception of the last term that differs because of the excess pore pressure profile (24) assumed in the present model.

3 SAMPLE CALCULATIONS

Here we present some results of the numerical solutions of the excess pore pressure diffusion equation (27) coupled with the streamwise depth-averaged momentum equation (28) and the Lagrangian form of the depth-averaged continuity equation used in Savage & Hutter (1989, 1991). The computational approach was the same as the Lagrangian scheme described in Savage & Hutter (1989, 1991). The purpose of these exploratory calculations was to gain some appreciation of the effects of fluid pore pressure and its diffusion on the development of debris flow surges.

The calculated flows are shown schematically in Figure 4. It was assumed that a fluid-solid mixture was initially contained on the slope by a vertical wall to form a wedge-shaped pile as indicated in Figure 4 at time $t = 0$. The material was released from rest on the rough

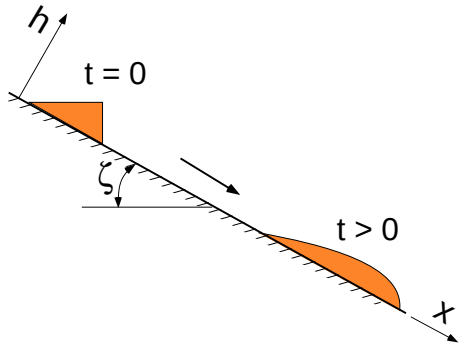

Figure 4: Schematic diagram of the release of a finite mass of debris on a rough incline.

incline and the flow velocities and surge shapes were determined at later times $t > 0$. The geometry and material parameters chosen for these calculations were similar to those of the USGS debris flow flume experiments. For example, the bed inclination angle $\zeta = 31°$, the solids bed friction angle $\delta = 28°$, and for the determination of $k_{actpass}$, the internal friction angle was chosen as $\phi = 42°$ (Iverson 1997). The characteristic lengths were taken to be $L = 5\text{m}$, and $H = 1.5\text{m}$. The initial condition for the bed pore pressure $p_b(x, t = 0)$ was assumed to be 85% of the value necessary for liquefaction of the material. By making use of (29), this provided the initial condition for the excess fluid pore pressure at the bed $\vartheta_b(x, 0)$.

As noted earlier, particle size segregation occurs during the surge process and moves the larger particles towards the snout of the debris flow resulting in a higher permeability and reduced excess pore pressures there. To account for this process in a very crude, but simple, way we have multiplied the diffusivity D_v appropriate for the debris flow material in the main part of the flow by the factor β.

$$\beta = 1 + c_1 \exp[-c_2(1 - \xi/l)]\,, \tag{31}$$

where c_1 and c_2 are constants, ξ is distance along the surge measured forward from the tail and l is the overall length of the surge from tail to nose. With values of $c_1 \sim 100$ and $c_2 \sim 10$, $\beta \simeq 1$ over most of the surge length, but is large near the nose region $\xi/l \to 1$.

Figures 5-8 show results of some calculations for dry material and for fluid-solid mixtures having various values of the physical pore pressure diffusivity D_v, and for $H = 1.5\text{m}$ and $L = 5.0\text{m}$. Figure 5 is for dry granular material and shows the profiles of depth h versus distance x for various times t. The initial wedge-shaped pile of material develops into a nearly parabolic profile as it moves downstream. Figures 6-8 are similar plots for fluid-solid mixtures having diffusivities D_v of $4{\times}10^{-3}$, $4{\times}10^{-4}$, and $4{\times}10^{-5}$ m^2/s respectively. These are comparable to the values of D_v measured in the USGS flume experiments which ranged from about $4{\times}10^{-4}$ to $4{\times}10^{-5}\text{m}^2/\text{s}$. The effects of the interstitial fluid and the diffusivity are clearly evident. In Figure 6, for the larger value of $D_v = 4 \times 10^{-3}\,\text{m}^2/\text{s}$, the excess pore pressure has dissipated to zero by a time $t \sim 4\text{s}$. The hydrostatic component of the pore pressure is still present. This reduces the solids bed friction below what would exist for dry material; thus, the debris mobility is enhanced. In Figure 7, for $D_v = 4 \times 10^{-4}\,\text{m}^2/\text{s}$, excess pore pressure is still finite over the middle region of the debris length for the last time shown, whereas in Figure 8, for $D_v = 4 \times 10^{-5}\,\text{m}^2/\text{s}$, the excess pore pressure is significant over most of the debris length at the last time frame of 8.57s.

The increase in diffusivity in the snout region, that was introduced as a crude way to handle the accumulation of large particles there, can strongly affect the development of the

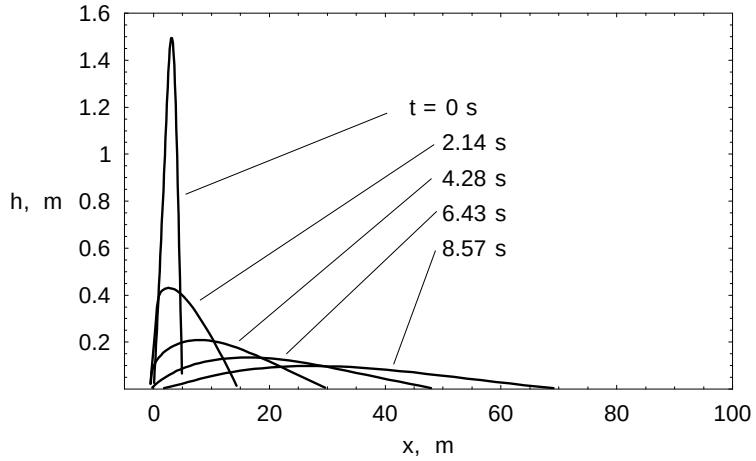

Figure 5: Depth profiles at successive times for case of dry granular material.

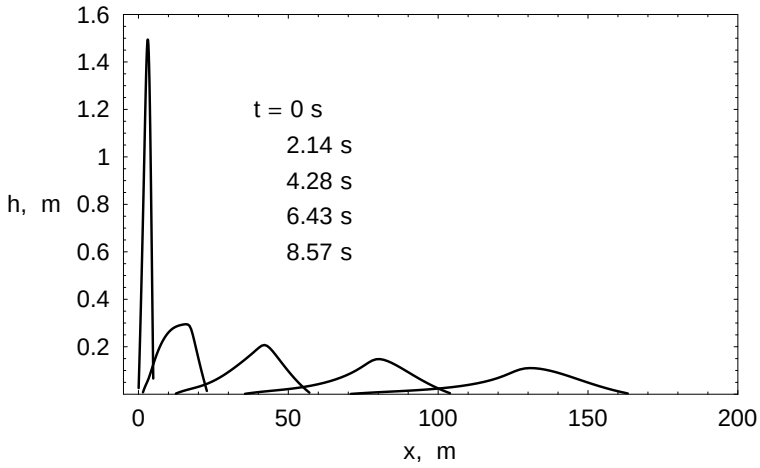

Figure 6: Depth profiles at successive times for fluid-solid mixture having $D_v = 4 \times 10^{-3}\,\mathrm{m}^2/\mathrm{s}$.

surge velocity and shape. The resulting decrease in excess pore pressure in the nose region, which effectively increases the solids bed friction, restrains the nose motion and causes the more mobile rear part of the flow to pile up against the snout region. This effect is more pronounced as the diffusivity over the main part of the debris is decreased.

4 CONCLUDING REMARKS

1. We have discussed a simple approach to consider the effects of diffusion of pore water pressure generated during the initial collapse and development of a debris flow surge.

2. The interstitial liquid was found to have strong effects on surge development. Its presence increases surge velocities and changes the depth profiles.

3. Decreases in the pore pressure diffusivity cause the pore pressures to decay more slowly, keep bed friction low and thereby increase the mobility of the surge.

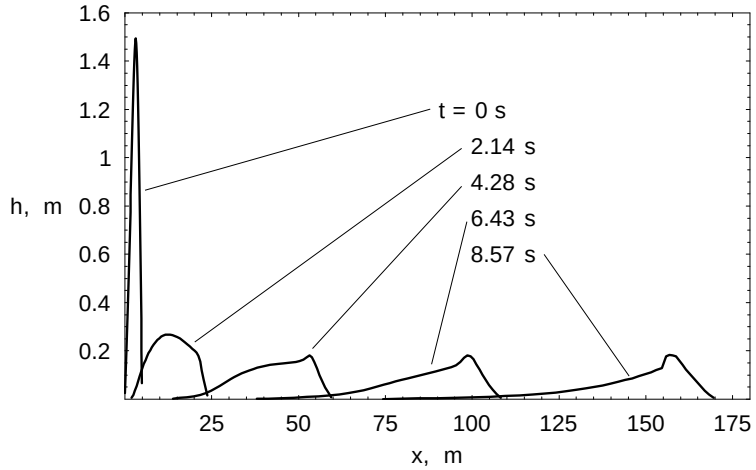

Figure 7: Depth profiles at successive times for fluid-solid mixture having $D_v = 4 \times 10^{-4}\,\mathrm{m}^2/\mathrm{s}$.

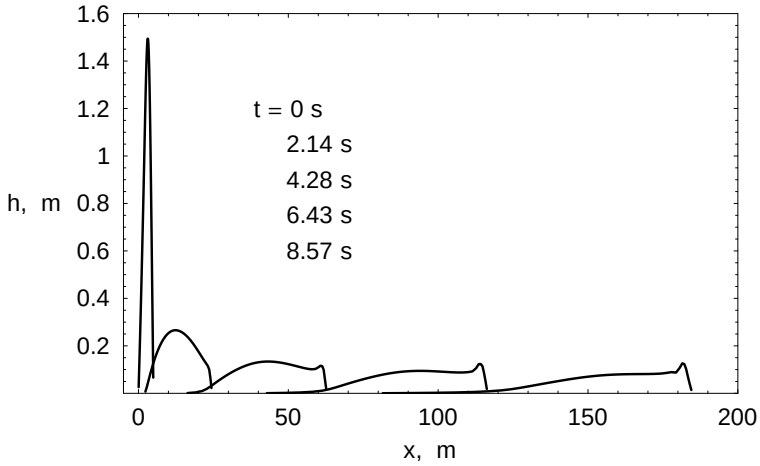

Figure 8: Depth profiles at successive times for fluid-solid mixture having $D_v = 4 \times 10^{-5}\,\mathrm{m}^2/\mathrm{s}$.

4. Both increased diffusivity at the nose of the surge arising from particle segregation and the lack of full saturation over depth can cause effective increases in bed friction at the surge leading edge and have profound effects on surge shapes and velocities. The detailed mechanics of the two-phase flow at the snout needs further study.

ACKNOWLEDGMENTS

S.B. Savage is grateful to the Natural Sciences and Engineering Research Council of Canada for the support of this work through an (NSERC) Research Grant.

REFERENCES

Bear, J. 1979. *Dynamics of Fluids in Porous Media.* New York: Elsevier.

Finlayson, B.A. 1972. *The Method of Weighted Residuals and Variational Principles.* New York: Academic Press, Inc.

Gidaspow, D. 1995. *Multiphase Flow and Fluidization.* San Diego: Academic Press, Inc.

Hutchinson, J.N. 1986. A sliding-consolidation model for flow slides. *Canadian Geotechnical Journal* 23: 115–126.

Iverson, R.M. 1997. The physics of debris flows. *Reviews of Geophysics* 35: 245–296.

Iverson, R.M. 2003. The debris-flow rheology myth. *This volume.*

Iverson, R.M. & Denlinger, R.P. 2001. Flow of variably fluidized granular masses across three-dimensional terrain: 1. Coulomb mixture theory. *Journal of Geophysical Research, B* 106: 537–552.

Savage, S.B. & Hutter, K. 1989. The motion of a finite mass of granular material down a rough incline. *Journal of Fluid Mechanics* 199: 177–215.

Savage, S.B. & Hutter, K. 1991. The dynamics of avalanches of granular materials from initiation to runout, Part I, analysis. *Acta Mechanica* 86: 201–223.

Savage, S.B. & Sayed, M. 1984. Stresses developed by dry cohesionless granular materials sheared in an annular shear cell. *Journal of Fluid Mechanics* 142: 391–430.

Scott, R.F. 1963. *Principles of Soil Mechanics.* Reading, Massachusetts: Adison-Wesley.

Suwa, H. 1988. Focusing mechanism of large boulders to a debris-flow front. *Japanese Geomorphological Union Transactions* 9: 151–178.

Takahashi, T. 1981. Debris flow. *Annual Review of Fluid Mechanics* 13: 57–77.

Terzaghi, K. 1963. *Theoretical Soil Mechanics.* New York: John Wiley & Sons.

Vallance, J.W. & Savage, S.B. 2000. Particle segregation in granular flows down chutes. In A. Rosato, and D. Blackmore (eds), *Segregation in Granular Flows, International Union of Theoretical and Applied Mechanics*: 31–51.